ACS APPLIED MATERIALS & INTERFACES

www.acsami.org

Research Article

Interwoven MOF-Coated Janus Cells as a Novel Carrier of Toxic Proteins

Laura Ha, Kyung Min Choi, and Dong-Pyo Kim*

Cite This: *ACS Appl. Mater. Interfaces* 2021, 13, 18545−18553

Read Online

ACCESS | Metrics & More | Article Recommendations | Supporting Information

ABSTRACT: Two major issues in cell-mediated drug delivery systems (c-DDS) are the availability of free cell surfaces for the binding of the cells to the target or to their microenvironment and internalization of the cytotoxic drug. In this study, the Janus structure, MOF nanoparticles, and tannic acid (TA) are utilized to address these issues. Janus carrier cells coated with metal−organic frameworks (MOFs) are produced by asymmetrically immobilizing the nanoparticles of a MOF based on zinc with cytotoxic enzymes that are internally encapsulated on the surface of carrier cells. By maintaining the biological and structural features of regular living cells, the MOF-coated Janus cells developed in the present study preserve the intrinsic binding capacity of the cells to their microenvironment. Interconnected MOFs loaded onto the other face of the Janus cells cannot penetrate the cell. Therefore, the carrier cells are protected from the cytotoxic drug contained in MOFs. These MOF-Janus carrier cells are demonstrated to successfully eliminate three-dimensional (3D) tumor spheroids when a chemotherapeutic protein of proteinase K is released from the MOF nanoparticles in an acid environment. The ease with which the MOF-Janus carrier cells are prepared (in 15 min), and the ability to carry a variety of enzymes and even multiple ones should make the developed system attractive as a general platform for drug delivery in various applications, including combination therapy.

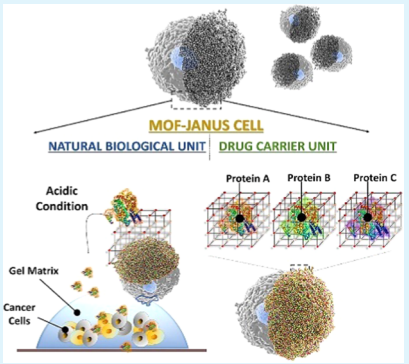

KEYWORDS: *cancer therapy, cell-mediated drug delivery, metal−organic frameworks, metal−phenolic networks, nanoparticle patch*

INTRODUCTION

Nanotechnology offers a promising strategy to improve the efficacy of various drugs to potentiate cancer therapy.[1] Among them, nanoscale metal−organic frameworks (MOFs), a class of hybrid materials developed via the self-assembly of metal ions and organic ligands, have emerged as a platform for the effective delivery of therapeutic drugs to tumor tissues.[2−4] Compared with other traditional porous materials, MOFs possess several obvious advantages such as high loading efficiency of drugs and biological macromolecules (DNA, and protein), tunable and designable functionality, stimuli-responsive degradability, and biocompatibility. With these unique properties, the MOF-based drug delivery system (DDS) has demonstrated an unprecedented opportunity for the treatment of cancer.[5−7] However, applications of MOF-based DDS are limited by their short in vivo circulation time and rapid phagocytic clearance.[8]

Recent years have witnessed significant effort dedicated to the development of novel drug delivery systems based on the living circulatory cells carrying drug-laden nanoparticles that link to the exterior surface of the cells.[9−14] Due to many attractive and distinctive features arising from circulatory cells, such as enhanced mobility, and a long circulation lifespan, the novel cell-mediated drug delivery systems (c-DDS) demonstrated enhanced drug carriage and controlled drug release.[8,9] For example, Mitragotri's group demonstrated the use of red blood cells (RBCs) as a carrier to prolong the resistance time of nanoparticles in blood.[15,16] Irvine et al. covalently attached drug-laden nanoparticles to therapeutic T cells and stem cells to activate T cells and increase the population of the stem cells in vivo.[17]

Although these systems take advantage of both the unique properties of the cells and the capabilities of the nanoparticles for enhanced drug loading and controlled drug release, these conventional methods still possess two major limitations. First, the interaction between nanoparticles and cell membrane leads to nanoparticle accumulation and subsequent internalization by phagocytosis or micropinocytosis.[18] This natural uptake mechanism of mammalian cells limits the type of therapeutic agents that can be carried by the circulatory cells because a drug with high cytotoxicity can induce cell death before reaching the target tissue.[19,20] To overcome the internalization problem, cellular backpacks, i.e., micron-scale patches a few hundred nanometers thick, were proposed.[21−23] Due to their microsize, the cellular backpacks are not engulfed by the carrier

Received: January 29, 2021
Accepted: April 6, 2021
Published: April 14, 2021

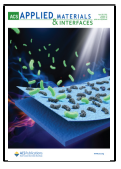

https://doi.org/10.1021/acsami.1c01927
ACS Appl. Mater. Interfaces 2021, 13, 18545−18553

cells. However, the fabrication involves a costly and time-consuming layer-by-layer (LbL) process, and yet the amount of the drug-laden "backpacks" that can be attached to the cell is limited. Second, cell-mediated drug delivery systems as reported are mostly designed to maximize drug loading capacity by randomly coating the drug-laden nanoparticles on the entire surface of the cells.[15,16] This complete and nonspecific blockage of the cell surface with the nanoparticle layer may prohibit the cell to physically interact with its microenvironment, hampering the cell binding with the target.

Here, we present a novel c-DDS system, termed MOF-coated Janus carrier cells, which resolves the problem of nanoparticle internalization and of the cell−microenvironment binding issue. MOF-coated Janus carrier cells are prepared by asymmetrically immobilizing the nanoparticles of a zinc-based MOF (ZIF-8, see the Material and Methods section) with cytotoxic enzymes encapsulated onto the surface of carrier cells (Scheme 1). Tannic acid (TA) is used to prevent the typical

Scheme 1. Schematic Illustration of the Development of MOF-Janus Cell-Based Drug Delivery System

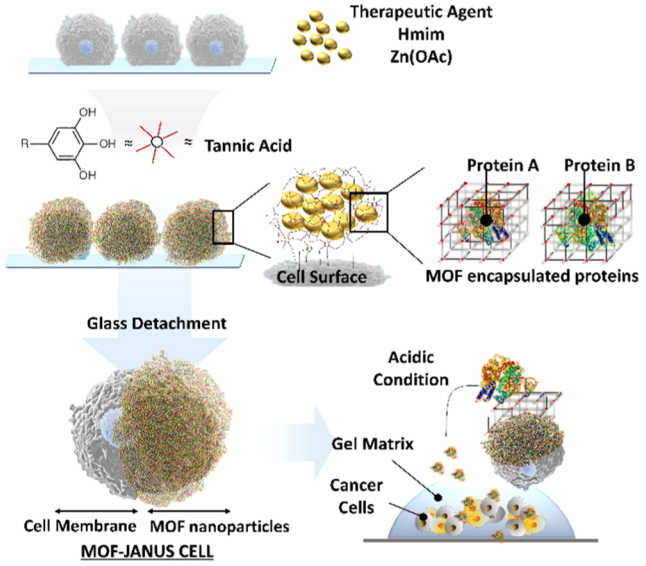

nanoparticle internalization pathway and to establish highly stable interactions between MOF nanoparticles and MOF-cell membranes via the multidentate tannic acid complexation.[24,25] By maintaining the biological and structural features of regular living cells, the MOF-coated Janus cells developed in the present study preserve the intrinsic binding capacity of the cells to their microenvironment. Furthermore, upon arriving at cancer cells, the MOF nanoparticles on the carrier cells quickly degrade and release the cytotoxic enzymes under acidic conditions, as described in the scheme.

RESULTS AND DISCUSSION

Validation of Stability of MOF Nanoparticles after Tannic Acid Application. From a DDS perspective, the stability of drug-laden MOF nanoparticles is a critical issue since the occurrence of unwanted leakage of the encapsulated drugs can seriously compromise the cell viability of the carrier. Therefore, before moving on to study the formation of MOF-coated Janus cell, the stability of MOF nanoparticles after TA application was examined in terms of nanoparticle morphology, crystallinity, and porosity.

The TA-coated ZIF-8 nanoparticles (ZIF-8-TA) were prepared by incubating ZIF-8 nanoparticles in the TA solution (0.4 mg/mL) for 10 min with gentle stirring. As shown in Figure 1A, ZIF-8 nanoparticles have an average size of 160 nm; Figure S1A shows the polydisperse particle size distribution. No conspicuous morphology alteration was observed after incubation of ZIF-8 nanoparticles in the TA solution (ZIF-8-TA) for 10 min. Furthermore, Figure 1B demonstrates that the crystallinity of ZIF-8 is little affected by the incubation. The change in porosity and pore size was also investigated via nitrogen adsorption−desorption measurements. In both ZIF-8 and ZIF-8-TA, steady N_2 adsorption at low relative pressure was observed (Figure 1C), and the Brunauer−Emmett−Teller (BET) surface areas of ZIF-8 and ZIF-8-TA are 1599 and 1574 m^2/g, respectively. Furthermore, as shown in Figure 1D, no transition of porous structures occurred due to the TA sculpturing process. These results illustrate that the stability of MOF nanoparticles is preserved even after the TA-assisted MOF coating on the cells. This conclusion is encouraging because the stability of nanoparticle capsules is critical for the safe protection of carrier cells against the cytotoxic effect of drug molecules.

Preparation of MOF-Coated Janus Cells. The MOF-coated Janus cells were developed as follows. A breast cancer cell line (MDA-MB-231 cell) was selected as a model circulatory cell since it has been shown homing back to their tumor of origin and been suggested as a good cancer cell-targeted drug delivery mediator.[26] First, the MDA-MB-231 cells attached to the ECM (extracellular matrix)-coated plate are interacted with ZIF-8 nanoparticles under aqueous conditions to facilitate the formation of multiple noncovalent bonding between the nanoparticles and cellular membrane components.[13,14] Then, TA, which is widely used for diverse pharmacological and biomedical applications,[25] is introduced to the system to achieve a highly stable multitude of MOF−cell membrane and MOF−MOF interactions via the multivalent tannic acid complexation.[27,28]

Figure S1B shows well-adhered nanoparticles on the cell surface. Energy-dispersive spectrometry (EDS) mapping reveals the uniform distribution of Zn^{2+} metal and confirms that the ZIF-8 nanoparticles are successfully attached to the cell surface. Fourier-transform infrared (FT-IR) spectroscopy was further performed on ZIF8 and TA-coated MDA-MB-231 cells to verify the formation of coordination bonds between TA and ZIF-8 nanoparticles (Figure S1C). Similar to the previous report by Zhu et al., the characteristic peaks at 1179 and 994 cm^{-1} assigned to the vibration of C═N and C−N in the imidazole ring of ZIF-8 and 1080 cm^{-1} assigned to the stretching vibration of C−O in tannic acid were examined, and the presence of TA and the zinc coordination bond was confirmed.[24] Next, confocal microscopy was used to verify the asymmetric coating of MOF nanoparticles (Figures 2A and S1D). For visualizing the location of MOF nanoparticles under a fluorescence microscope, FITC-labeled MOF nanoparticles were used. Figure 2A shows that the MOF nanoparticles are asymmetrically attached to the particles. The cell viabilities of MDA-MB-231 cells after the asymmetric surface modification were 85.2, 82.4, and 88.8% for 0, 24, and 48 h after coating, respectively (Figure 2B).

When these MOF-coated carrier cells are removed from the plate, MOF-coated Janus cells contain the parts of the cells that were in contact with the plate becoming the bare face of the Janus structure. These collected Janus cells were examined

https://doi.org/10.1021/acsami.1c01927
ACS Appl. Mater. Interfaces 2021, 13, 18545−18553

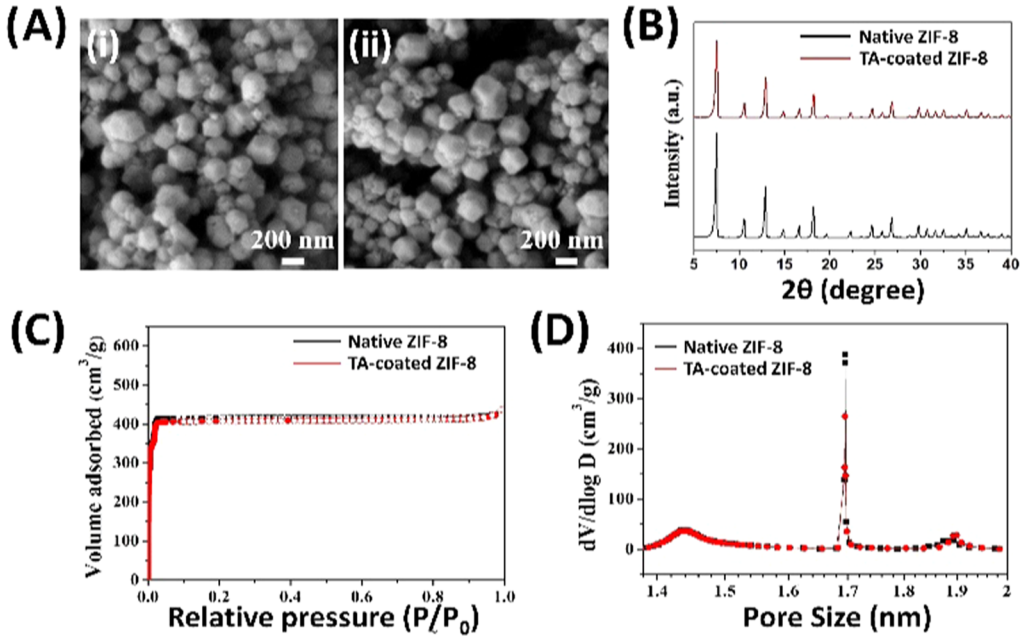

Figure 1. Verification of tannic acid (TA)-derived decomposition of ZIF-8 nanoparticles. High-resolution scanning electron microscopy (HR-SEM) micrograph of (A-i) native ZIF-8 and (A-ii) TA-coated ZIF-8 (scale bar: 200 nm). (B) X-ray diffraction (XRD) spectra of ZIF-8 and TA-coated ZIF-8. (C) The N_2 adsorption graph of native ZIF and tannic acid-coated ZIF-8. (D) Pore size distribution of native ZIF-8 and tannic acid-coated ZIF-8.

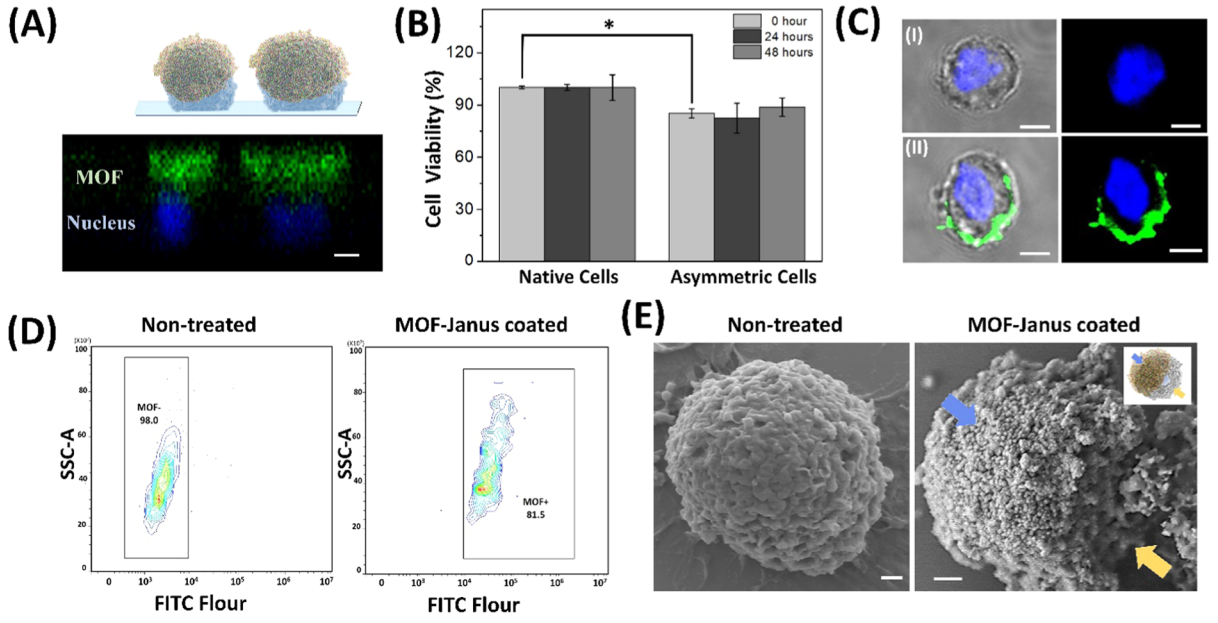

Figure 2. Development of MOF-coated Janus cells. (A) The Z-stacked confocal micrographic image of ZIF-8 coated glass adherent cells (blue: cell nucleus, green: FITC-labeled ZIF-8, scale bar: 5 μm). (B) Cell viability assay of glass adherent mammalian cells coated with ZIF-8 nanoparticles. (C) Confocal micrographs of (C-I) native cell (C-II) Janus cell (scale bar: 5 μm). (D) Flow cytometry analysis of Janus cells carrying FITC-labelled ZIF-8 nanoparticles. (E) SEM micrograph of the native cell and the MOF nanoparticle patch attached onto the Janus cell (bar: 1 μm). The p value in (B) was calculated using the t-test (***$p < 0.001$, **$p < 0.01$, * $p < 0.05$).

under a fluorescence microscope and SEM. The asymmetric fluorescence signal originating from MOF was maintained in the free-floating MOF-coated cells, as shown in Figure 2C. Flow cytometry analysis demonstrated that over 80% of the collected Janus cells carried FITC-labelled MOF nanoparticles as shown in Figure 2D. Interestingly enough, the SEM micrograph in Figure 2E reveals the nanoparticle presence as a form of a microsized patch on the cell surface. It is noted in this regard that, unlike the conventional microsized backpack, the developed nanoparticle patch makes conformal contact around the curved cell surface, which indicates more stable attachment of the drug on the carrier cells with the help of TA.[21−23]

Ability of Microenvironment Binding and Transmigration across the Endothelial Monolayer. In circulatory cells such as blood circulating tumor cells, or T-cells, membrane proteins such as integrin proteins have a central role in extravasation and transmigration across the endothe-

https://doi.org/10.1021/acsami.1c01927
ACS Appl. Mater. Interfaces 2021, 13, 18545−18553

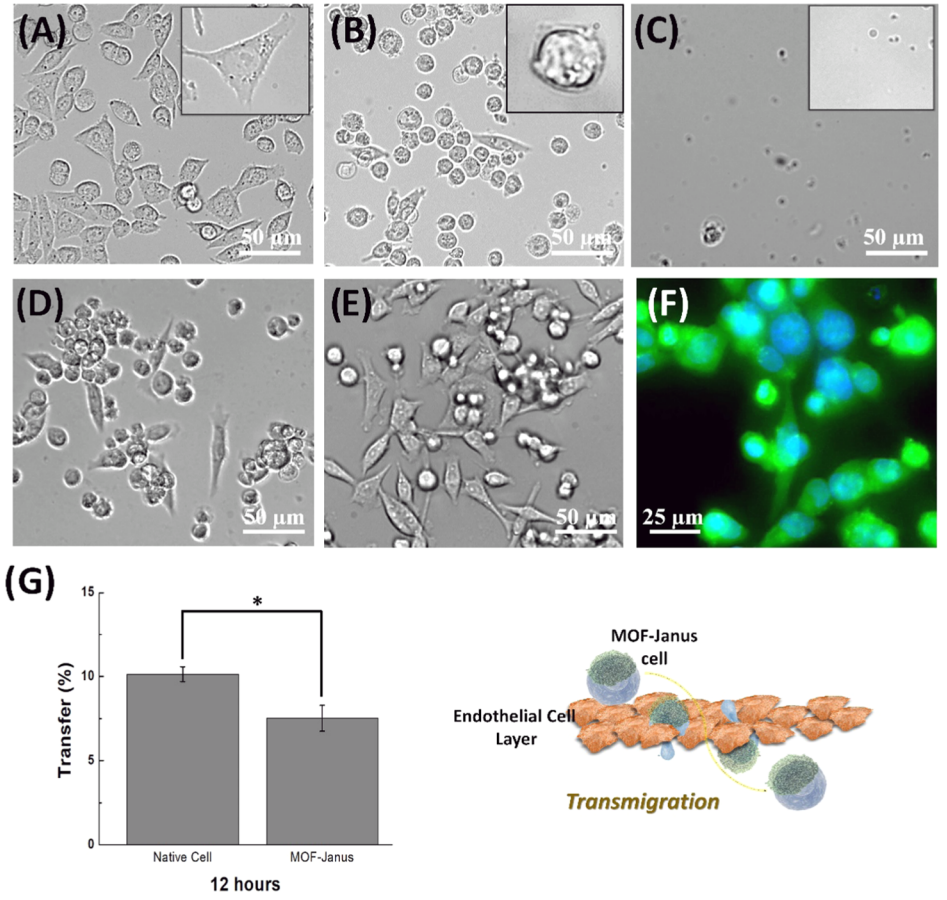

Figure 3. Integrin-mediated cell−microenvironment interactions. The micrograph of glass adherent (A) native cells, (B) MOF-Janus cells, and (C) ZIF-8 fully coated cells. The microscopic image of MOF-Janus cells incubated with DMEM at (D) neutral pH and (E) at pH 6 for 1 h. (F) Viability of MOF-Janus cells after removal of the ZIF-8 nanoparticles at pH 6. (G) In vitro assay of the translocation of native MDA-MB-231 cells and MOF-Janus cells across endothelial cell monolayers. The p value in (G) was calculated using the t-test (***$p < 0.001$, **$p < 0.01$, *$p < 0.05$).

lium or lymph node.[29−31] Despite the importance of the aforementioned integrin protein, however, the conventional design of c-DDS has attempted to fully conjugate the drug molecules on the cell surface.[15−17,21−23] Unlike the conventional design, the MOF-coated Janus cells developed in our study preserve the biological and structural features of the MDA-MB-231 cells. In Figure 3, comparisons are made between the naked MDA-MB-231 cells, Janus cells, and MDA-MB-231 cells coated with ZIF-8 nanoparticles on the entire surface for the cell−microenvironment interaction. The cells were seeded on an ECM-coated commercial 12 well plates separately and incubated in a CO_2 incubator at 36 °C with cell culture media and 5% fetal bovine serum for 6 h. After washing the cells multiple times with phosphate-buffered saline (PBS), the cell attachment on the substrate was examined with a microscope.

Figure 3A−C shows that the naked MDA-MB-231 cells and Janus cells are well attached on the substrate but the cells fully coated with ZIF-8 nanoparticles are barely attached on the substrate. Differences in morphology were observed between the naked cells and Janus cells. The attached Janus cells typically maintained a confined shape, while the naked cells exhibited an elongated and stretched shape. This restricted morphology of the Janus cells might be due to the rigid ZIF-8 nanoparticles coated on the cell membrane tightly gripping the cell.

To verify that degradation of MOF does not affect the morphology and viability of the Janus cell, the MOF coated on the cell was decomposed by placing the Janus cell in acidic culture media at pH 6 for 1 h; then the media was exchanged with the fresh cell culture media at neutral pH. Upon removing the ZIF-8 nanoparticles, the Janus cells started to stretch and become elongated like native MDA-MB-231, while the untreated Janus cells retained the round morphology (Figure 3D,E). The recovered cell viability was also verified by a cell-permeable fluorescent probe, calcein AM, that interacts with the esterase present in the healthy cell cytoplasm. As seen in Figure 3F, the Janus cells showed good cell viability even after the removal of ZIF-8 nanoparticles (Figure S2).

A preliminary in vitro test was also carried out to show whether Janus cells were able to cross an endothelial cell monolayer. Janus cells were incubated in transwell plates containing a cell monolayer of human endothelial cells (HUVEC) and chemoattractant, hEGF, that was placed in the lower chamber.[32] As shown in Figure 3G, Janus cells as well as native MDA-MB-231 cells can across the HUVEC cell monolayer in vitro, although the number of Janus cells that were transferred across the monolayer was slightly lower than that of native MDA-MB-231 cells.

Delivery of Proteinase K to the In Vitro Cancer Model. Confirmations of the successful formation and performance evaluation of Janus cells prompted us to test its potential use in cytotoxic drug delivery and cancer targeting.

https://doi.org/10.1021/acsami.1c01927
ACS Appl. Mater. Interfaces 2021, 13, 18545−18553

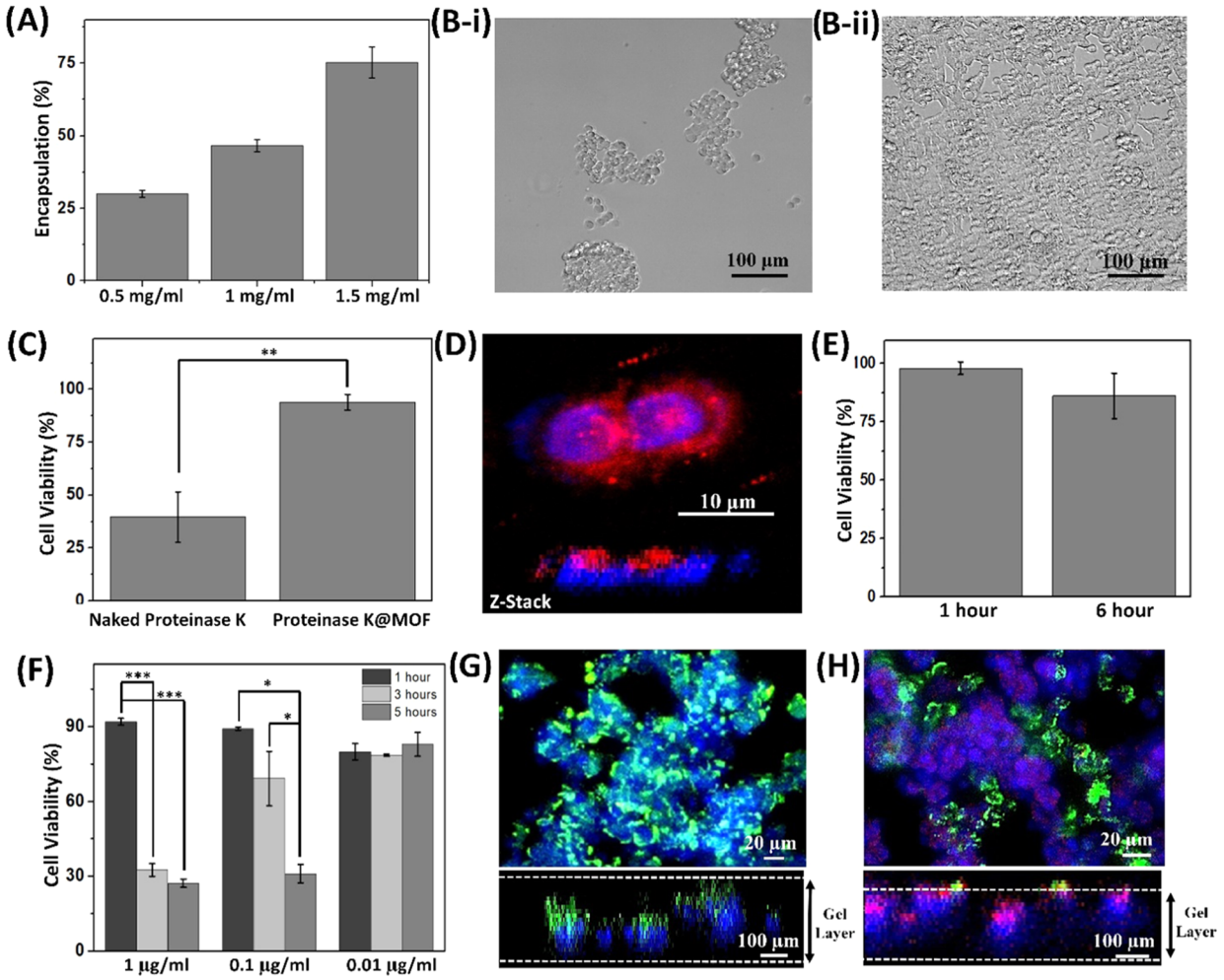

Figure 4. In vitro drug delivery and cancer spheroid targeting of MOF-Janus cells. (A) Encapsulation efficiency of various concentrations of proteinase K in ZIF-8 nanoparticles. Microscopic images of cells treated with (B-i) native proteinase K and (B-ii) the proteinase K@MOF nanoparticle for an hour. (C) Percent cell viability after treatment with native proteinase K or the proteinase K@MOF nanoparticle for 1 h. (D) Confocal micrograph of proteinaseK@MOF attached on cells (blue: cell nucleus, red: proteinase K). (E) Cell viability of MOF-Janus cells after attachment of proteinase K on its surface for 1 and 6 h. (F) Target breast cancer tissue viability after coincubating with MOF-Janus cells containing different concentrations of proteinase K for 1, 3, and 5 h. (G) Cell viability of Matrigel-embedded MDA-MB-231 (green: live cells, red: dead cells, blue: all cell nuclei). (H) MOF-Janus cells targeting site attachment and release of proteinase K to kill Matrigel-embedded MDA-MB-231 (green: MOF-Janus cells, red: dead cell nuclei, blue: all cell nuclei). The p values in (C) and (F) were calculated using the t-test (***$p < 0.001$, **$p < 0.01$, *$p < 0.05$).

For this purpose, proteinase K, a nonspecific serine protease known to quickly digest cell surface proteins and lyse cells, was selected as a mock drug that is delivered to the target cancer tissue. Before proceeding to the test, however, a number of points need to be checked and clarified. Of interest, for instance, is the amount of proteinase K encapsulated by MOF, or encapsulation efficiency defined by the percentage of proteinase K successfully entrapped into the MOF nanoparticles. A one-pot synthesis method was used to prepare proteinase K-containing MOF of ZIF-8 (proteinase K@MOF) by adding 0.07 mg/mL $Zn(OAc)_2$(aq.) to an aqueous solution of 2-methylimidazole (Hmim; 0.1 g/mL) that contains various concentrations of proteinase K; the morphology of proteinase K-encapsulated MOF nanoparticles was examined under an SEM (Figure S3A). The particle size of proteinase K@MOF was a bit larger than that of native ZIF-8, which might be attributed to the influence of the enzyme on the process of nucleation and growth of ZIF-8.[33] The amount captured or encapsulated by MOF was determined by decomposing the MOF in an acidic solution and then using UV−vis and Bradford assay for the quantification with the help of a standard curve generated with known concentrations of proteinase K (Figure S3B). Figure 4A shows that the efficiencies, on average, are 30.0, 46.6, and 75.2% for 0.5, 1, and 1.5 mg/mL concentration of proteinase K, respectively; note that the encapsulation efficiency of protein-concentration-dependent increase was similar to that of previous report.[34]

Cell viability in the presence of bare proteinase K and proteinase K contained in MOF nanoparticles was probed by introducing them to MDA-MB-231 cells attached to a glass substrate. For this purpose, the proteinase K@MOF nanoparticles containing 0.15 mg of proteinase K were dispersed in (i) 1 mL of serum-free cell culture media and (ii) 0.15 mg of only bare proteinase K dispersed in the same media. Within an hour, most of the cells incubated with bare proteinase K were detached from the glass substrate (Figure 4B-i). However, the MDA-MB-231 cells incubated with proteinase K@MOF nanoparticles established stable attachment on their substrate

https://doi.org/10.1021/acsami.1c01927
ACS Appl. Mater. Interfaces 2021, 13, 18545−18553

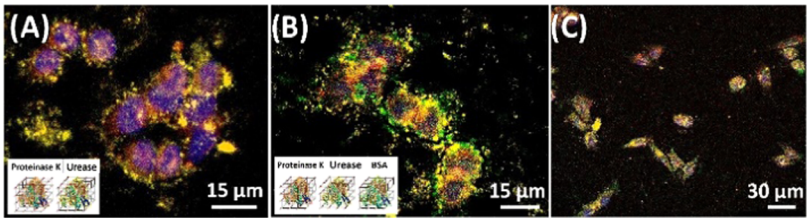

Figure 5. Multiproteins loading onto the MOF-Janus carrier cells. (A) Dual-protein loading on carrier cells. (B, C) Triple-protein loading on carrier cells in two different magnifications (red: proteinase K, green: BSA, yellow: urease, blue: cell nucleus).

(Figure 4B-ii). The viability as determined by the MTS assay was 39.7% for the bare proteinase K exposed group and 93.9% for the proteinase K@MOF exposed group (Figure 4C). These results confirm stable encapsulation of proteinase K inside MOF nanoparticles and successful blockage of direct interaction between proteinase K enzyme and MDA-M-231 cells.

Figure 4D shows TA-assisted stable binding of proteinase K@MOF on the cells identified via confocal micrography. For better visualization of the proteinase K location on the cells, proteinase K was labeled with Cy5 fluorophore prior to MOF encapsulation and attachment on the cell surfaces. The total amount of proteinase K attached per 1×10^6 cells was calculated to be 0.167 mg; 14.8% of the total amount of proteinase K@MOF treated were loaded per 1×10^6 of carrier cells.

The protection of the MDA-MB-231 carrier cells against the cytotoxic drug, which is afforded by MOF, was checked by incubating the carrier cells coated with MOF nanoparticles containing proteinase K in a CO_2 incubator with serum-free cell culture media. The MTS assay was performed to quantify the cell viability and bare MOF-nanoparticles-linked cells were used as a control. Figure 4E shows that the cell viability was 98.1 and 86.2% after 1 and 6 h, respectively, confirming successful carrier cell protection against the drug toxicity. The cell viability of whole coated cells was 74.6% after 6 h (Figure S4A). The slight decrease in cell viability for a longer incubation time was presumed to be due to the release of loosely bound proteinase K on the surface of the MOF nanoparticles.

To finally test the MOF-Janus cell-based c-DDS for cancer therapy, the release behavior of proteinase K from MOF and the dosage requirement were examined. For the release behavior, proteinase K@ZIF-8 containing 0.15 mg of proteinase K was dissolved in DMEM at pH 6, the pH known to be prevalent in extracellular and interstitial space of tumors, and the amount of protein in the solution was measured over time using UV−vis and Bradford assay (Figure S4B). A 100% protein release was observed within 60 min. Although the release behavior would depend on pH, this trend of fast dissolution of ZIF-8 nanoparticles is similar to that reported earlier.[35]

To optimize the dosage, three batches of Janus cells containing 1, 0.1, and 0.01 μg/mL each of proteinase K were introduced to the confluent monolayer of MDA-MB-231 cells (2D breast cancer tissue) cultured in 96 well plates. To mimic the cancer microenvironment, cell culture media was adjusted to pH 6, and cell viability was quantified by MTS assay over time. Figure 4F shows that the percent viability of 2D breast cancer tissue subjected to the Janus cells of 1 μg/mL proteinase K decreased from 92.0% in 1 h to 32.5 and 27.2% in 3 and 5 h, respectively. When the dosage was decreased to 0.1 μg/mL, the corresponding percent viabilities were 89.2, 69.2, 30.9% for 1, 3, and 5 h of incubation, respectively. When it was further decreased to 0.01 μg/mL, no significant change in the cell viability was observed; the cell viabilities were 79.9, 78.5, and 80.9% for 1, 3, and 5 h of incubation, respectively.

For an in vivo-like cancer therapy, three-dimensional (3D) tumor spheroids were produced by culturing MDA-MB-231 mixed with Matrigel via the hanging drop technique.[36] After 2 days of incubation in a CO_2 incubator, the spheroid formation was observed under a microscope. The viability of the developed tumor spheroids in Matrigel was confirmed with calcein AM and propidium iodide (PI) staining as shown in Figure 4G. When the Janus cells containing 1 μg/mL proteinase K were introduced to the cancer spheroids system, stable attachment of the Janus cells on the surface of the cancer spheroids embedding Matrigel was observed (Figure S5). Once the tumor extracellular environment-like condition was mimicked in the system, rapid death of tumor spheroid cells and the Janus cells occurred within 3 h (Figure 4H). These results demonstrate the toxic therapeutic protein delivery effectiveness and cancer targeting efficiency of the c-DDS developed here.

Development of Multiprotein-Loaded Janus Cells. The ability to carry and deliver a variety of enzymes and even multiple enzymes should help establish the Janus cells as a general platform for cell-mediated drug delivery. For a demonstration, MOFs encapsulating proteinase K, urease, and bovine serum albumin (BSA) were prepared, each labeled with different fluorescent dyes (Figure S6). A simple mixing of the protein containing MOFs with mammalian cells and subsequent TA-assisted binding led to cells loaded with multiple enzymes. Figure 5 shows the results of successful co-loading on the cells of two proteins and three proteins of BSA@MOF, proteinase K@MOF, and urease@MOF, respectively. This ability to carry multiple enzymes in the MOF of the Janus cell DDS developed here bodes well for combination therapy, a treatment modality that combines two or more therapeutic agents as a cornerstone of cancer therapy that has drawn great interest.[37−40]

CONCLUSIONS

In summary, Janus carrier cells coated with interwoven MOFs only on one face of the Janus structure have been developed as a cell-mediated DDS. The interwoven MOFs on the carrier cells cannot be internalized, resulting in the protection of the carrier cells from the cytotoxic proteins contained in the MOFs. Interaction of the carrier cells with the target cells is assured by the bare face of the Janus cells. The cytotoxic proteins in the MOFs are released when the MOFs reach the target cells in an acidic environment. Effective elimination of cancer cells has been quantitatively confirmed by introducing the proteinase K-containing MOF-Janus cells to in vivo-like

https://doi.org/10.1021/acsami.1c01927
ACS Appl. Mater. Interfaces 2021, 13, 18545−18553

cancer environment. The entire process of preparing Janus cells takes less than 15 min, including the synthesis of drug-laden MOF nanoparticles, asymmetric attachment of the nanoparticles to the cell surface, and detachment of the MOF-coated cells from the substrate. The ability of the MOF-Janus cells to deliver a variety of proteins and even multiple enzymes makes the system suitable for a general platform for cell-mediated drug delivery. It also opens the door to co-delivery applications, including combination therapy.

MATERIALS AND METHODS

Preparation of Fluorophore-Labeled Proteins. Proteinase K, BSA, and urease were separately prepared by labeling each protein with Cy5, FITC, and Cy5.5 fluorophores. Briefly, the enzyme of interest was first dissolved in PBS (1×; pH 7.4) at 1 mg/mL. Subsequently, 4 μL of the sulfo-fluorophore-NHS ester (1 mM; Lumiprobe) was added and incubated for 30 min. Then, the modified proteins were purified three times with PBS through a 100 kDa filter (Millipore) with centrifugation at 3600 rpm for 10 min.

Synthesis of Enzyme-Encapsulated or -Unencapsulated ZIF-8 Nanoparticles. 2-Methylimidazole (Hmim, 0.1 g/mL) dissolved in 1× PBS was added to an equal volume of 0.07 g/mL zinc acetate ($Zn(OAc)_2$(aq.)) dissolved in 1× PBS. After stirring for 10 min at room temperature, the particles were collected by centrifuging at 10 000 rpm for 5 min. The collected particles were washed with ethanol and water several times. For the synthesis of enzyme-encapsulated ZIF-8, the enzyme of interest was added to 0.1 g/mL Hmim and 0.07 g/mL $Zn(OAc)_2$(aq.). After stirring for 10 min at room temperature, the particles were collected via repeated centrifuging and washing with ethanol and water.

Tannic Acid Binder-Assisted ZIF-8 Coating on Living Cells (ZIF-8/TA-Coated Cells) and Formation of MOF-Janus Cells. The coating of ZIF-8 nanoparticles on living cells was performed following the previously reported method with slight modifications.[19] Briefly, approximately 1×10^5 MDA-MB-231 cells were plated in 12 well plates and cultured in Dulbecco modified Eagle's medium (DMEM) at 37 °C in a humidified 5% CO_2 incubator. After reaching 80% confluence, the cells were rinsed with 1× PBS, and then 500 μL of 20 mg/mL ZIF-8 nanoparticles that were monodispersed in 1× PBS solution was added to the cells. After 15 s of gentle shaking, 500 μL of 32 μg/mL tannic acid in 1× PBS solution was added into the system for 30 s. Then, the unbound ZIF-8 nanoparticles were removed from the system via repeated washing with DMEM. The formation of MOF-Janus cells was achieved via introducing trypsin (0.25 mg/mL) into the ZIF-8-coated cells for 3 min with gentle shaking. The detached cells were collected through centrifugation and fresh DMEM was introduced into the MOF-Janus cells. The formation of ZIF-8-coated MOF-Janus cells was confirmed using an LSM 700 microscope (Zeiss, Axio Observer) and flow cytometry (BD CytoFLEX).

Chemotaxis Assay. Migratory activities of Janus cells were investigated using an in vitro model of the confluent monolayer of HUVEC cells that were grown on poly(ethylene terephthalate) (PET; 8 μm pore) inserts. FITC-labeled Janus cells (1.5×10^5 cells/mL), suspended in a medium (50% DMEM, 50% EBM, 0.1% bovine serum albumin), were added into the HUVEC cells contained in the upper chambers. Native MDA-MB-231 cells were used as a control. We loaded EGF, a well-known cancer cell chemoattractant, into the lower chamber.[20] Following incubation for 12 h in 5% CO_2 at 37 °C, the cell inserts were removed. Cells in the bottom chamber were collected and counted. The Janus cell percent transfer across the HUVEC monolayers was calculated by subtracting the number of retrieved Janus cells from the original. Each experiment was triplicated.

Formation of Multiprotein-Loaded MOF-Janus Cells. MOF-encapsulated enzymes were separately prepared via mixing fluorescent-labeled proteinase K, BSA, and urease with ZIF-8 precursors. The collected nanoparticles were resuspended in fresh DMEM; equal volumes of different ZIF-8-encapsulated MOFs were mixed together. Then, 500 μL of mixed ZIF-8 nanoparticle-encapsulated enzymes were added to the MDA-MB-231 cells containing 12 well plates. After 15 s of gentle shaking, 500 μL of 32 μg/mL tannic acid in 1× PBS solution was added into the system for 30 s. Then, the unbound ZIF-8 nanoparticles were removed from the system via repeated washing with DMEM. The formation of ZIF-8-coated MOF-Janus cells was confirmed using an LSM 700 microscope (Zeiss, Axio Observer).

Determination of Proteinase K Encapsulation Efficiency and Release Profile by UV−Vis Spectroscopic Analysis. The SDS-washed proteinase K-encapsulated ZIF-8 nanoparticles were suspended in 1 mL of citric acid (pH 6) for 6 h to release encapsulated protein via acidic decomposition. The resulting solution was treated using an ultrafiltration device (Millipore, 100 kDa). After washing two times with ultrapure water, the resulting solution (100 μL) was mixed with 1 mL of Bradford solution (Sigma-Aldrich), and the solution was incubated for 5 min at room temperature. The spectra were collected on a UV-2550 spectrometer (Shimadzu, Japan). The encapsulation efficiency of the protein was calculated using the ratio of absorbance of protein collected from the protein-encapsulating ZIF-8 nanoparticles to the absorbance of proteins of the concentration initially provided in the reaction mixture for the synthesis of proteinase K@MOF nanoparticles. For the determination of the release profile, the washed samples were incubated in citric acid (pH 6). Every 5−10 min, 100 μL of the sample solution was withdrawn and mixed with 1 mL of the Bradford solution. The amount of proteins released from the MOF nanoparticles was determined using a UV-2550 spectrometer (595 nm). All of the experiments were performed in triplicate. The overall amount of the protein content of the biocomposite was then compared with the amount of protein obtained by dissolution.

Quantification of the Amount of Proteinase K Loading on the Carrier Cells. MDA-MB-231 cells (1×10^6) were cultured in each well of the 12 well plates. Approximately, 20 mg of MOFs containing proteinase K was introduced to each well, and an asymmetric coating of proteinase K@MOF on the cells was carried out. The unbound MOF nanoparticles were collected from the supernatant and the nanoparticles were decomposed in the citrate phosphate solution (pH 6) for 6 h. The amount of the retrieved protein was measured using the UV−vis and Bradford assay. The amount of proteinase K loading on the carrier cells was calculated by subtracting the amount of retrieved proteinase K from the original amount of proteinase K treated with 1×10^6 MDA-MB-231 cells. Each experiment was performed in triplicate.

Delivery of Proteinase K with MOF-Janus Cells to 2D Breast Cancer Cell Tissue and Cancer Spheroid and Cell Viability Assay. Two-dimensional (2D) breast cancer tissue was prepared by seeding 1×10^4 MDA-MB-231 cells into the 96 well plates. Once a confluent monolayer of tissue was formed, MOF-Janus cells with proteinase K at concentrations of 1, 0.1, and 0.01 μg/mL were introduced into each well. To induce the release of proteinase K from MOF nanoparticles, fresh DMEM at pH 6 was introduced to the system. The cancer tissue viability at different incubation times was measured using an MTS assay kit. As a control, the 2D breast cancer tissue incubated with the same number of MOF-Janus cells without proteinase K was used. All of the experiments were performed in triplicate. The formation of the cancer spheroid was performed as a 3D tissue model. Briefly, Matrigel (Corning) was first diluted with DMEM containing 5% FBS, 1× Pen Strep to a final concentration of 0.1 mg/mL. One milliliter of the diluted Matrigel was mixed with $(8-10) \times 10^5$ MDA-MB-231 cells. Using a 100 μL pipette, 30 μL of drops were added to the bottom of the 24 well plates. The well plate was inverted and incubated at 37 °C/5% CO_2 overnight allowing gel formation. After 2 days of incubation in a CO_2 incubator, with FBS containing cell culture media, MOF-Janus cells with proteinase K at a concentration of 1 μg/mL were introduced into the system and cocultured for 4 h. Then, to induce the release of proteinase K from MOF nanoparticles, fresh DMEM at pH 6 was added to the system. The cancer tissue viability at different incubation times was examined via live/dead assay with calcein AM and PI staining. A confocal microscope was used for the visualization of the live and dead cells. Z-

https://doi.org/10.1021/acsami.1c01927
ACS Appl. Mater. Interfaces 2021, 13, 18545−18553

stacking was performed to further examine the location of dead cells in the 3D gel.

Characterization of ZIF-8-Coated Cells by Scanning Electron Microscopy. ZIF-8-coated MOF-Janus cells were fixed with 2.5% glutaraldehyde (Sigma-Aldrich). Then, the cells were sequentially dehydrated with 25, 50, 75, 85, 95, and 100% ethanol solution in PBS. Then, they were completely freeze-dried overnight. The sample was sputtered with Pt prior to imaging. SEM micrographs of the sample were taken using a high-resolution FE-SEM at an accelerating voltage of 10.0 keV.

Statistical Analysis. The statistical significance of the obtained results was determined using Student's *t*-test. A significance level was chosen at a minimum p value of 0.05.

■ ASSOCIATED CONTENT

Supporting Information

The Supporting Information is available free of charge at https://pubs.acs.org/doi/10.1021/acsami.1c01927.

SEM images; FT-IR spectra; XRD crystal structure model; and photographs of Janus cells (PDF)

A 3D-confocal video of the Janus cells demonstrating asymmetric coating of MOF on the cell surfaces (AVI)

■ AUTHOR INFORMATION

Corresponding Author

Dong-Pyo Kim − *A Center for Intelligent Microprocess of Pharmaceutical Synthesis Department of Chemical Engineering, Pohang University of Science and Technology (POSTECH), Pohang 37673, Republic of Korea;* orcid.org/0000-0003-4676-9766; Phone: +82 10 6758 0125; Email: dpkim@postech.ac.kr

Authors

Laura Ha − *A Center for Intelligent Microprocess of Pharmaceutical Synthesis Department of Chemical Engineering, Pohang University of Science and Technology (POSTECH), Pohang 37673, Republic of Korea*

Kyung Min Choi − *Department of Chemical and Biological Engineering and Institute of Advanced Materials & Systems, Sookmyung Women's University, Yongsan-gu, Seoul 04310, Republic of Korea*

Complete contact information is available at: https://pubs.acs.org/10.1021/acsami.1c01927

Notes

The authors declare no competing financial interest.

■ ACKNOWLEDGMENTS

Valuable discussions and technical assistance for BET analysis from Dong Chang Kang are gratefully acknowledged. This work was supported by the National Research Foundation (NRF) of Korea, funded by the Korean government (NRF-2017R1A3B1023598).

■ REFERENCES

(1) Nam, J.; Son, S.; Park, K. S.; Zou, W.; Shea, L. D.; Moon, J. J. Cancer Nanomedicine for Combination Cancer Immunotherapy. *Nat. Rev. Mater.* **2019**, *4*, 398−414.

(2) Furukawa, H.; Cordova, K. E.; O'keeffe, M.; Yaghi, O. M. The Chemistry and Applications of Metal−Organic Frameworks. *Science* **2013**, *341*, No. 1230444.

(3) Giancotti, F. G.; Ruoslahti, E. Integrin Signaling. *Science* **1999**, *285*, 1028−1033.

(4) Ni, K.; Lan, G.; Lin, W. Nanoscale Metal−Organic Frameworks Generate Reactive Oxygen Species for Cancer Therapy. *ACS Cent. Sci.* **2020**, *6*, 861−868.

(5) Liang, K.; Ricco, R.; Doherty, C. M.; Styles, M. J.; Bell, S.; Kirby, N.; Mudie, S.; Haylock, D.; Hill, A. J.; Doonan, C. J.; Falcaro, P. Biomimetic Mineralization of Metal−Organic Frameworks as Protective Coatings for Biomacromolecules. *Nat. Commun.* **2015**, *6*, No. 7240.

(6) Liang, K.; Coghlan, C. J.; Bell, S. G.; Doonan, C. J.; Falcaro, P. Enzyme Encapsulation in Zeolitic Imidazolate Frameworks: A Comparison Between Controlled Co-precipitation and Biomimetic Mineralization. *Chem. Commun.* **2016**, *52*, 473−476.

(7) Poddar, A.; Conesa, J. J.; Liang, K.; Dhakal, S.; Reineck, P.; Bryant, G.; Pereiro, E.; Ricco, R.; Amenitsch, H.; Doonan, C.; Mulet, X.; Doherty, C. M.; Falcaro, P.; Shukla, R. Encapsulation, Visualization and Expression of Genes with Biomimetically Mineralized Zeolitic Imidazolate Framework-8 (ZIF-8). *Small* **2019**, *15*, No. 1902268.

(8) Rosenblum, D.; Joshi, N.; Tao, W.; Karp, J. M.; Peer, D. Progress and Challenges Towards Targeted Delivery of Cancer Therapeutics. *Nat. Commun.* **2018**, *9*, No. 1410.

(9) Agrahari, V.; Agrahari, V.; Mitra, A. K. Next Generation Drug Delivery: Circulatory Cells-Mediated Nanotherapeutic Approaches. *Expert Opin. Drug Delivery* **2017**, *14*, 285−289.

(10) Liu, J.; Guo, Z.; Li, Y.; Liang, J.; Xue, J.; Xu, J.; Whitelock, J. M.; Xie, L.; Kong, B.; Liang, K. pH-Gated Activation of Gene Transcription and Translation in Biocatalytic Metal−Organic Framework Artificial Cells. *Adv. NanoBioMed. Res.* **2021**, *1*, No. 2000034.

(11) Liu, J.; Guo, Z.; Liang, K. Biocatalytic Metal−Organic Framework-Based Artificial Cells. *Adv. Funct. Mater.* **2019**, *29*, No. 1905321.

(12) Ji, Z.; Zhang, H.; Liu, H.; Yaghi, O. M.; Yang, P. Cytoprotective metal−organic frameworks for anaerobic bacteria. *Proc. Natl. Acad. Sci. U.S.A.* **2018**, *115*, 10582−10587.

(13) Liang, K.; Richardson, J. J.; Doonan, C. J.; Mulet, X.; Ju, Y.; Cui, J.; Caruso, F.; Falcaro, P. An Enzyme-Coated Metal−Organic Framework Shell for Synthetically Adaptive Cell Survival. *Angew. Chem.* **2017**, *129*, 8630−8635.

(14) Liang, K.; Richardson, J. J.; Cui, J.; Caruso, F.; Doonan, C. J.; Falcaro, P. Metal−Organic Framework Coatings as Cytoprotective Exoskeletons for Living Cells. *Adv. Mater.* **2016**, *28*, 7910−7914.

(15) Chambers, E.; Mitragotri, S. Prolonged Circulation of Large Polymeric Nanoparticles by Non-covalent Adsorption on Erythrocytes. *J. Controlled Release* **2004**, *100*, 111−119.

(16) Chambers, E.; Mitragotri, S. Long Circulating Nanoparticles via Adhesion on Red Blood Cells: Mechanism and Extended Circulation. *Exp. Biol. Med.* **2007**, *232*, 958−966.

(17) Stephan, M. T.; Moon, J. J.; Um, S. H.; Bershteyn, A.; Irvine, D. J. Therapeutic Cell Engineering with Surface-conjugated Synthetic Nanoparticles. *Nat. Med.* **2010**, *16*, 1035−1041.

(18) Fleischer, C. C.; Payne, C. K. Nanoparticle−Cell Interactions: Molecular Structure of the Protein Corona and Cellular Outcomes. *Acc. Chem. Res.* **2014**, *47*, 2651−2659.

(19) Verma, A.; Stellacci, F. Effect of Surface Properties on Nanoparticle−Cell Interactions. *Small* **2010**, *6*, 12−21.

(20) Nel, A. E.; Madler, L.; Velegol, D.; Xia, T.; Hoek, E. M. V.; Somasundaran, P.; Klaessig, F.; Castranova, V.; Thompson, M. Understanding Biophysicochemical Interactions at the Nano-bio Interface. *Nat. Mater.* **2009**, *8*, 543−557.

(21) Shields, C. W.; Evans, M. A.; Wang, L. L. W.; Baugh, N.; Mitragotri, S.; et al. Cellular Backpacks for Macrophage Immunotherapy. *Sci. Adv.* **2020**, *6*, No. eaaz6579.

(22) Klyachko, N. L.; Polak, R.; Haney, M. J.; Zhao, Y.; Neto, R. J. G.; Hill, M. C.; Kabanov, A. V.; Cohen, R. E.; Rubner, M. F.; Batrakava, E. V. Macrophages with Cellular backpacks for Targeted Drug Delivery to the Brain. *Biomaterials* **2017**, *140*, 79−87.

(23) Xia, J.; Wang, Z.; Huang, D.; Ran, Y.; Li, Y.; Guan, J. Asymmetric Biodegradable Microdevices for Cell-Borne Drug Delivery. *ACS Appl. Mater. Interfaces* **2015**, *7*, 6293−6299.

(24) Zhu, W.; Guo, J.; Amini, S.; Ju, Y.; Agola, J. O.; Zimpel, A.; Shang, J.; Noureddine, A.; Caruso, F.; Wuttke, S.; Croissant, J. G.; Brinker, C. J. SupraCells: Living Mammalian Cells Protected within Functional Modular Nanoparticle-Based Exoskeletons. *Adv. Mater.* **2019**, *31*, No. 1900545.
(25) Rahim, M. A.; Ejima, H.; Cho, K. L.; Kempe, K.; Mullner, M.; Best, J. P.; Caruso, F. Coordination-Driven Multistep Assembly of Metal−Polyphenol Films and Capsules. *Chem. Mater.* **2014**, *26*, 1645−1653.
(26) Parkins, K. M.; Dubois, V. P.; Kelly, J. J.; Chen, Y.; Knier, N. N.; Foster, P. J.; Ronald, J. A. Engineering Circulating Tumor Cells as Novel Cancer Theranostics. *Theranostics* **2020**, *10*, 7925−7937.
(27) Ejima, H.; Richardson, J. J.; Liang, K.; Best, J. P.; van Koeverden, M. P.; Such, G. K.; Cui, J.; Caruso, F. One-Step Assembly of Coordination Complexes for Versatile Film and Particle Engineering. *Science* **2013**, *341*, 154−157.
(28) Zhu, W.; Xiang, G.; Shang, J.; Guo, J.; Motevalli, B.; Durfee, P.; Agola, J. O.; Coker, E. N.; Brinker, C. J. Versatile Surface Functionalization of Metal−Organic Frameworks through Direct Metal Coordination with a Phenolic Lipid Enables Diverse Applications. *Adv. Funct. Mater.* **2018**, *28*, No. 1705274.
(29) Hogg, N.; Laschinger, M.; Giles, K.; McDowall, A. T-cell Integrins: More than Just Sticking Points. *J. Cell Sci.* **2003**, *116*, 4695−4705.
(30) Desgrosellier, J. S.; Cheresh, D. A. Integrins in Cancer: Biological Implications and Therapeutic Opportunities. *Nat. Rev. Cancer* **2010**, *10*, 9−22.
(31) Hamidi, H.; Ivaska, J. Every Step of the Way: Integrins in Cancer Progression and Metastasis. *Nat. Rev. Cancer* **2018**, *18*, 533−578.
(32) Sun, R.; Gao, P.; Chen, L.; Ma, D.; Wang, J.; Oppenheim, J. J.; Zhang, N. Protein Kinase C zeta Is Required for Epidermal Growth Factor−Induced Chemotaxis of Human Breast cancer Cells. *Cancer Res.* **2005**, *65*, 1433−1441.
(33) Wu, X.; Ge, J.; Yang, C.; Hou, M.; Liu, Z. Facile synthesis of multiple enzyme-containing metal−organic frameworks in a biomoleculefriendly environment. *Chem. Commun.* **2015**, *51*, 13408−13411.
(34) Zhu, G.; Cheng, L.; Qi, R.; Zhang, M.; Zhao, J.; Zhu, L.; Dong, M. A metal−organic zeolitic framework with immobilized urease for use in a tapered optical fiber urea biosensor. *Microchim. Acta* **2020**, *187*, No. 72.
(35) (a) Carraro, F.; Vel′asquez-Hern′andez, M. D. J.; Astria, E.; Liang, W.; Twight, L.; Parise, C.; Ge, M.; Huang, Z.; Ricco, R.; Zou, X.; Villanova, L.; Kappe, C. O.; Doonan, C.; Falcaro, P. Phase dependent encapsulation and release profile of ZIF-based biocomposites. *Chem. Sci.* **2020**, *11*, 3397−3404. (b) Badea, M. A.; Balas, M.; Hermenean, A.; Ciceu, A.; Herman, H.; Ionita, D.; Dinischiotu, A. Infuence of Matrigel on Single- and Multiple-Spheroid Cultures in Breast Cancer Research. *SLAS Discovery* **2019**, *24*, 563−578.
(36) Hu, C. M. J.; Zhang, L. Nanoparticle-based Combination Therapy Toward Overcoming Drug Resistance in Cancer. *Biochem. Pharmacol.* **2012**, *83*, 1104−1111.
(37) Valencia, P. M.; Pridgen, E. M.; Perea, B.; Gadde, S.; Sweeney, C.; Kantoff, P. W.; Bander, N. H.; Lippard, S. J.; Langer, R.; Karnik, R.; Farokhzad, O. C. Synergistic Cytotoxicity of Irinotecan and Cisplatin in Dual-Drug Targeted Polymeric Nanoparticles. *Nanomedicine* **2013**, *8*, 687−698.
(38) Jia, J.; Zhu, F.; Ma, X. H.; Cao, Z. W. W.; Li, Y. X. X.; Chen, Y. Z. Mechanisms of Drug Combinations: Interaction and Network Perspectives. *Nat. Rev. Drug Discovery* **2009**, *8*, 111−128.
(39) Chou, T.-C. Theoretical Basis, Experimental Design, and Computerized Simulation of Synergism and Antagonism in Drug Combination Studies. *Pharmacol. Rev.* **2006**, *58*, 621−681.
(40) Sabnis, A. J.; Bivona, T. G. Principles of Resistance to Targeted Cancer Therapy: Lessons from Basic and Translational Cancer Biology. *Trends Mol. Med.* **2019**, *25*, 185−197.

https://doi.org/10.1021/acsami.1c01927
ACS Appl. Mater. Interfaces 2021, 13, 18545−18553